Journal of Catalysis 276 (2010) 327–334

Contents lists available at ScienceDirect

Journal of Catalysis

journal homepage: www.elsevier.com/locate/jcat

Direct synthesis of carbon-templating mesoporous ZSM-5 using microwave heating

Jeong-Boon Koo [a], Nanzhe Jiang [a], Shunmugavel Saravanamurugan [a], Martina Bejblová [b], Zuzana Musilová [b], Jiří Čejka [b,*], Sang-Eon Park [a,*]

[a] Laboratory of Nano-Green Catalysis and Nano Center for Fine Chemicals Fusion Technology, Department of Chemistry, Inha Univ., Incheon 402-751, Republic of Korea
[b] J. Heyrovsky Institute of Physical Chemistry, Academy of Sciences of the Czech Republic, v.v.i., Dolejskova 3, CZ-182 23 Prague 8, Czech Republic

ARTICLE INFO

Article history:
Received 28 April 2010
Revised 8 August 2010
Accepted 23 September 2010
Available online 25 October 2010

Keywords:
Mesoporous ZSM-5
Template
Microwave irradiation
Carbon
Acidity
2′,4′-dimethoxyacetophenone

ABSTRACT

Carbon-templated mesoporous ZSM-5 zeolites were synthesized directly avoiding a drying process. Carbon nanoparticles were simply mixed into synthesis precursor of ZSM-5 and hydrothermally treated by microwave irradiation. The amount of mesopores formed inside the ZSM-5 single crystals was controllable by adjusting the amount of carbon used. For comparison, mesoporous ZSM-5 zeolites have also been synthesized under hydrothermal conditions. The influence of microwave irradiation on mesoporous ZSM-5 materials was thoroughly investigated by using nitrogen adsorption/desorption studies and ^{27}Al MAS NMR. The nature of acid sites both in the micropores (internal) and on the surface of mesopores (external) was investigated by in situ FTIR spectroscopy using pyridine (Py) and 2′,6′-di-tert-butylpyridine (DTBPy) as a probe molecules. Mesoporous ZSM-5 prepared by microwave synthesis showed higher catalytic activity in the bulky molecular reaction of 2′,4′-dimethoxyacetophenone (2′,4′-DMAP) with 4-methoxybenzaldehyde as a model reaction in comparison with the results obtained over hydrothermally prepared ZSM-5. The further catalytic behavior has been studied in condensation reaction and cracking of substituted benzene.

1. Introduction

Zeolites (crystalline microporous aluminosilicates) are the most important heterogeneous acid catalysts in oil refinery, petrochemistry and fine chemical synthesis due to the strong acidity, shape selectivity and high hydrothermal stability [1–4]. Small pore size (<1 nm) limits further catalytic applications of zeolites particularly in transformations of bulky substrates. From that reason, different synthesis approaches have been investigated to increase the accessibility of bulky molecules to the active sites of zeolite materials [5–8]. Particularly, mesoporous zeolites have been attracted a great interest in the catalytic applications due to the diffusional alleviation of reactants molecules and high thermal stability. Several strategies are available to prepare hierarchical mesoporous and microporous materials [9–12], but still some challenges have to be fulfilled for the commercial requirements such as cost, facile preparation and control of the location of the active sites. In order to access the internal pores, the mesopores could be created within the zeolite crystals by post-synthesis treatments such as dealumination, desilication and other chemical treatments [12,13]. Dual templating methods have also been applied for the synthesis of mesoporous zeolites with the co-presence of zeolitic template and hard templates such as carbon and polymer or organic surfactants as supramolecular soft-templates [14,15].

There are numerous reports on the synthesis of mesoporous zeolites by carbon templating method which is relatively facile and inexpensive. The mesoporous zeolites were prepared by nucleating the zeolite crystals around the carbon particles [16]. Mesoporous carbon CMK-3 was used as a precursor for the preparation of mesoporous ZSM-5 zeolite [17] and carbon aerogel for the synthesis of ZSM-5 crystals with bimodal pore structure of uniform mesoporous channels [18,19]. Jacobsen et al. found that by using excess of a zeolite gel, it was possible to grow zeolite around the carbon particles to obtain large single crystals [16]. The uniform carbon particles created mesopores after removal of carbon by calcination. Therefore, the resulted mesopores in the zeolite crystals were indeed induced by the carbon templating. Under an excessive amount of carbon particles, zeolite crystals nucleated restrictedly in mesopore system of carbon particles, whereas low amount let the zeolite crystals grow over the carbon particles. Usually, drying process is adopted in carbon templating method for removing water from synthesis precursor before hydrothermal treatment [17,18].

Recently, microwave-assisted heating has been considered as a useful method in the hydrothermal synthesis of various types of nanoporous materials including zeolites, mesoporous silica and their composites [20,21]. Microwave-irradiated heating not only provides distinct advantages over the conventional synthesis such

* Corresponding authors. Fax: +420 28658 2307 (J. Čejka), fax: +82 32 8728670 (S.-E. Park).
E-mail addresses: jiri.cejka@jh-inst.cas.cz (J. Čejka), separk@inha.ac.kr (S.-E. Park).

0021-9517/$ - see front matter © 2010 Elsevier Inc. All rights reserved.
doi:10.1016/j.jcat.2010.09.024

as rapid heating, homogeneous nucleation, supersaturation by the rapid dissolution of precipitated gels and a shorter crystallization time but also is efficient for mesopore generation by desilication [22–25]. Most recently, we encapsulated metal oxide nanoparticles into the carbon-templated mesoporous MFI zeolites directly during microwave synthesis [26]. The carbon particles were considered not only as a hard template but also as a good microwave absorber [27,28]. In this way, the general evaporation process before thermal treatment of the synthesis precursor was skipped.

In the present study, we report on the synthesis of mesoporous ZSM-5 zeolite crystals directly from the normal synthesis gel of ZSM-5 under efficient and controlled microwave heating varying the amount of carbon added as secondary template. For comparison, mesoporous ZSM-5 zeolites were also synthesized from the same reaction gel under conventional hydrothermal conditions. The mesoporosity of the materials was controlled by varying the amount of carbon in the synthesis gel. The influence of the microwave irradiation on the physicochemical properties of mesoporous ZSM-5 has been thoroughly investigated by combining nitrogen adsorption/desorption measurements, ^{27}Al MAS NMR and in situ FTIR spectroscopy. Specially, in the FTIR, the internal and external acid sites were discriminated by using Py and DTBPy as probe molecules. The catalytic behavior of mesoporous ZSM-5 zeolites was investigated in the reaction of 2′,4′-dimethoxyacetophenone (2′,4′-DMAP) with 4-methoxybenzaldehyde in the absence of any solvent. The catalytic behavior has been studied in condensation reaction and cracking of substituted benzene. The catalytic activity was compared with standard ZSM-5 zeolite.

2. Experimental

2.1. Synthesis of materials

The chemicals used for the preparation of materials were tetraethyl orthosilicate (TEOS) (Aldrich, 98%), aluminum nitrate (Aldrich, 98%), tetra-n-propylammonium hydroxide (TPAOH) (TCI, 25%) as a template for ZSM-5 and Carbon Black Pearls 2000 (Cabot Corporation) as a hard template. The molar composition of the mixture was 1.0:34.6:53.4:982 = Al:Si:TPAOH:H_2O. In a typical synthesis, aluminum nitrate was dissolved in distilled water. TEOS was mixed with ethanol and added to the above solution. After stirring the reaction mixture for 90 min, aqueous solution of TPAOH was added. The whole mixture was further vigorously stirred for 2 h, and appropriate amount of carbon ranging from 0 to 40 wt.% related to C/Si source (corresponding sample denoted as MW-0, to MW-40) was added and allowed to stir for another 5 h. The resulted mixture was subjected to microwave digestion (MARS-5, CEM Products) system. The microwave condition was set at 80 °C for 30 min and 165 °C for 1 h with an operating power of 600 W at 170 psi. In the case of hydrothermal synthesis, the mixture was transferred to Teflon-coated autoclave and heated at 170 °C for 6 days under static condition (sample signed as HT-0 to HT-40). The prepared solid was filtered off, washed out with distilled water and dried at ambient temperature. The carbon and organic templates were then removed by stepwise calcination in air flow at 550 °C for 10 h. The calcined ZSM-5 was ion-exchanged with 100 ml/g of 0.5 M NH_4NO_3 solution four times at room temperature under agitation for 5 h. The solid material was filtered off, washed out with deionized water and dried at 100 °C for 6 h. The NH_4-form zeolite was calcined at 550 °C to get H form.

2.2. Characterization

The powder X-ray diffraction (XRD) patterns were obtained on a Rigaku diffractometer using Cu Kα radiation (λ = 0.154 nm). The powder patterns were recorded in the 2θ range of 0.7–3° at the rate of 1.0°/min (40 kV and 20 mA) and in the 2θ range of 5–60° at the rate of 3.0°/min (30 kV, 15 mA). Nitrogen adsorption/desorption studies were conducted on a Micromeritics ASAP 2020 surface area and pore size analyzer at −196 °C. The surface areas were calculated using BET method, and the pore parameters were determined from desorption branches by BJH methods. Scanning electron

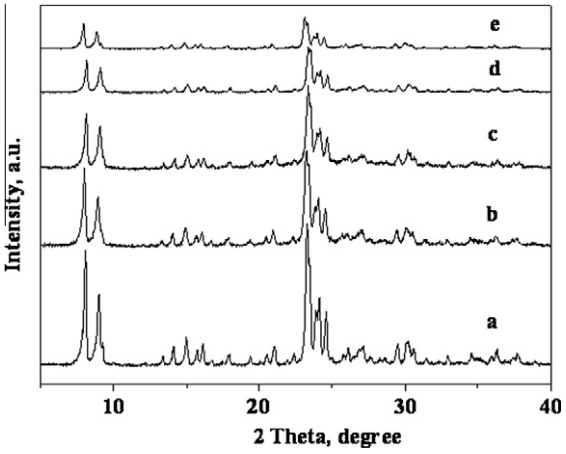

Fig. 1. XRD patterns of mesoporous ZSM-5 synthesized by microwave (a) MW-0, (b) MW-10, (c) MW-20, (d) MW-30, (e) MW-40.

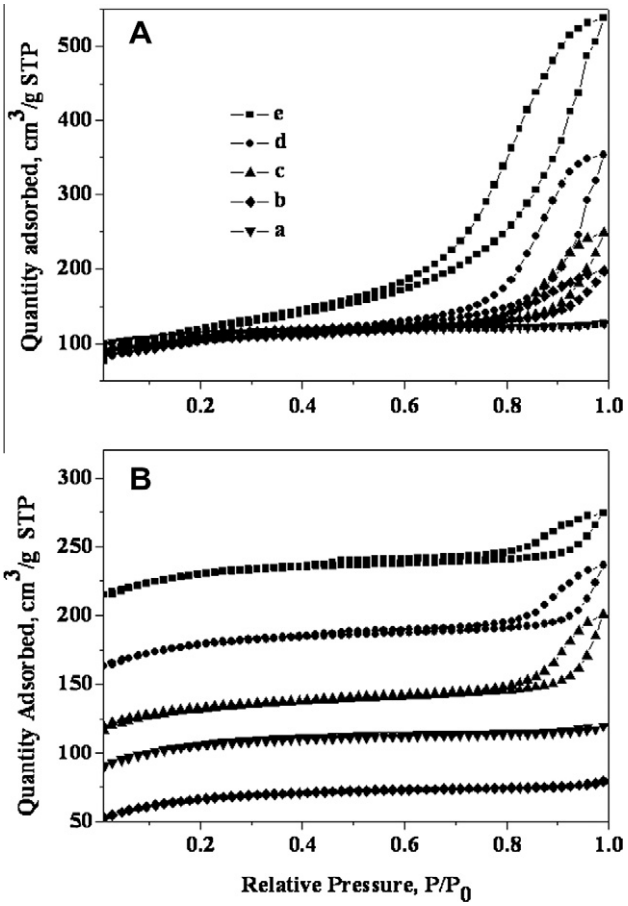

Fig. 2. N_2 adsorption/desorption isotherms of mesoporous ZSM-5 synthesized by (A) microwave (a) MW-0, (b) MW-10, (c) MW-20, (d) MW-30, (e) MW-40; (B) hydrothermal (a) HT-0, (b) HT-10, (c) HT-20, (d) HT-30, (e) HT-40.

Table 1
Physicochemical properties of mesoporous ZSM-5 synthesized by microwave.

Catalysts	BET surface area (m^2/g)	Micropore area (m^2/g)	Mesopore area (m^2/g)	Micropore volume (cm^3/g)	Mesopore volume (cm^3/g)
MW-0	352	249	92	0.13	0.06
MW-10	339	183	197	0.06	0.24
MW-20	340	122	154	0.09	0.29
MW-30	336	135	217	0.07	0.49
MW-40	398	78	383	0.04	0.82
HT-0	358	259	88	0.13	0.06
HT-10	359	249	104	0.13	0.07
HT-20	367	266	102	0.14	0.15
HT-30	361	250	111	0.13	0.14
HT-40	328	216	112	0.11	0.12

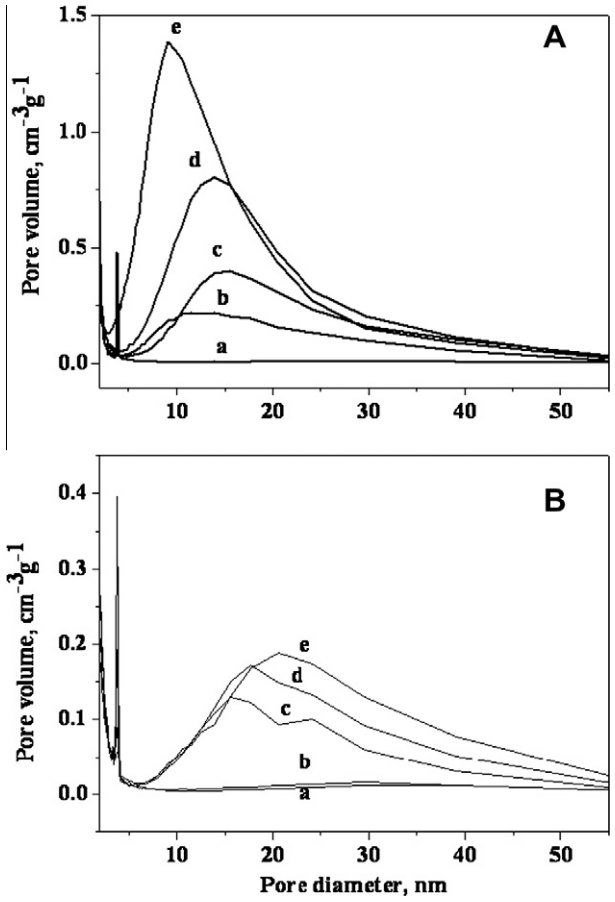

Fig. 3. Pore size distribution of mesoporous ZSM-5 materials (A) microwave (a) MW-0, (b) MW-10, (c) MW-20, (d) MW-30, (e) MW-40; (B) hydrothermal (a) HT-0, (b) HT-10, (c) HT-20, (d) HT-30, (e) HT-40.

microscopy images were obtained with Hitachi S-4200 at 15–20 kV. Transmission electron microscopy images were taken using a Philips CM 200 at 200 kV. ^{27}Al MAS NMR spectra were recorded on 400 MHz solid state Avance II Bruker NMR with spinning rate of 13 kHz and delay time of 1 s. Adsorption of Py proceeded at 150 °C at partial pressure of 1000 Pa for 30 min, followed by desorption at 150 °C for 20 min. All spectra were recorded with a resolution of 2 cm^{-1} by collecting 128 scans for a single spectrum and were recalculated on wafer thickness of 10 mg/cm^2. From the integral intensities of individual adsorption bands at 1545 cm^{-1} (Brønsted acid sites) and at 1450 cm^{-1} (Lewis acid sites) and using extinction coefficients (ε_B = 1.67 ± 0.1 cm/μmol, ε_L = 2.22 ± 0.1 cm/μmol), concentration of Brønsted and Lewis acid sites was determined. The adsorption of DTBPy proceeded at 150 °C by equilibrating the catalyst wafer with the probe vapor pressure for 15 min followed by 1-h degassing at the same temperature and by collection of the spectrum at room temperature. For the determination of concentration of Lewis and Brønsted acid sites, extinction coefficients for pyridine were used.

2.3. Catalytic reaction

Twenty millimoles of 2′,4′-DMAP, 20 mmol of 4-methoxybenzaldehyde and 100 mg of the catalyst (activated at 150 °C under vacuum) were charged into the reaction vessel. The reaction mixture was stirred at 140 °C for 24 h under inert atmosphere. Products were analyzed by gas chromatography (Agilent 5890 N equipped with HP-5 column).

Condensation reactions of acetophenone were performed in the liquid phase under batch conditions. In a typical reaction, catalysts (100 mg) were activated for 2 h at 100 °C and added to acetophenone (40 mmol), and the resulting suspension was magnetically stirred at 160 °C.

Catalytic cracking of 1,3,5-triisopropylbenzene was carried out in the fixed bed reactor. The catalytic testing was performed according to the following standard conditions: the mass of the catalyst was 0.2 g, reaction temperature was 673 K, 0.2 mL of 1,3,5-triisopropylbenzene was injected per 1 h into the catalyst bed with nitrogen carrier gas at a flow rate of 200 mL/min.

3. Results and discussion

3.1. Crystallinity of MFI type crystals

In general, the XRD patterns of carbon-templated zeolites provide a lower intensity than conventional ZSM-5 (without carbon), which could be explained in terms of a lower density of mesoporous in zeolite crystals [29]. The XRD patterns (Fig. 1) of all zeolites synthesized by conventional hydrothermal (not shown) and microwave methods revealed MFI structure after the combustion of carbon template. However, the intensity of the peaks was slightly reduced by increasing carbon amounts in the synthesis precursor. The carbon particles could interfere to reduce the intensity of the peaks due to the mesopore voids formed in the ZSM-5 crystals after the removal of carbon. It was due to the formation of disordered mesopores within the single zeolite crystals which may cause the formation of defects.

3.2. Dependence of textural properties on carbon content

Fig. 2 provides nitrogen adsorption and desorption isotherms of carbon-templated zeolites synthesized by both microwave and conventional hydrothermal methods. Microwave-synthesized zeolites showed the hysteresis loops appearing from relative pressure of P/P_0 = 0.6 (Fig. 2A) confirming the presence of mesopores in the

ZSM-5 crystals. The hydrothermally synthesized zeolites showed the hysteresis loops from relative pressure of $P/P_0 = 0.8$ (Fig. 2B) being higher than as for microwave-synthesized zeolites and predict the formation of larger mesopores. The amount of nitrogen adsorbed on mesoporous ZSM-5 zeolites depends on the amount of carbon added into the precursor gel for both synthesis methods, and the dependency is more straightforward for the microwave-synthesized zeolites. The mesopore surface area of mesoporous ZSM-5 zeolites prepared by microwave increased from 197 to 383 m^2/g; in parallel, micropore pore volume decreased from 0.13 to 0.04 cm^3/g (Table 1). Hydrothermal method provides mesopore surface area from 88 to 112 m^2/g but no big changes in micropore pore volume from 0.13 to 0.11 cm^3/g (Table 1). It apparently indicated that the pore volume of the mesoporous ZSM-5 zeolites prepared by conventional hydrothermal method was much less than that of zeolites prepared by microwave (Table 1). Moreover, the carbon particles did not play a significant role to create the mesopores within the zeolite crystals under hydrothermal conditions. It might be due to a longer hydrothermal crystallization time, during which the aggregation of carbon particles could be possible, and the aggregated carbon particles settled down at the bottom of the vessel. But in the case of microwave method, carbon particles play very important role. We suggested that it is because of the carbon materials playing a role as microwave absorber [21,23,26]. It can be inferred that microwave heating activated carbon surface and enhanced the interaction of carbon particles with the silica source in the synthesis solution enhancing the rate of crystallization [30–32].

The hydrothermally synthesized mesoporous ZSM-5 zeolites revealed the presence of interparticle void volume in the range of 5–55 nm with the maximum at about 20 nm (Fig. 3A). As already mentioned, the carbon did not play a significant role to create mesopores in ZSM-5 crystals. But microwave effect gives more narrowed pore size distribution of real mesopores in the range of 5–40 nm with the maximum at about 10 nm; it is close to the size of the carbon particles (Fig. 3B). The distribution width was reduced compared with earlier reports [16,29]. The absorption of microwave by carbon particles was of paramount importance to generate mesopores within the zeolite crystals at rather short synthesis times.

3.3. Dependence of textural properties on carbon content

The SEM images of the mesoporous ZSM-5 zeolites prepared by microwave (MW-0 to MW-40) are illustrated in Fig. 4. The scanning electron micrographs of the calcined samples showed typical form of crystals. The crystal sizes of the samples were 0.8–1 μm. The surface of typical ZSM-5 crystals MW-0 was smooth, whereas in the case of mesoporous ZSM-5 crystals from MW-10 to MW-40, the surface was uneven because of voids left by nanosized carbon particles [33]. These voids stem from the fact that carbon particles are accidentally distributed inside and outside of zeolite crystals.

The TEM images of MW-0 to MW-40 are shown in Fig. 5. Fig. 5A revealed that there are no mesopores in MW-0 prepared without carbon, whereas Fig. 5B–E the dotted bright parts could be recognized as mesopores. The TEM images clearly showed the presence of disordered mesopores within the ZSM-5 crystals, which are accessible only through the microporous channels of ZSM-5 domains.

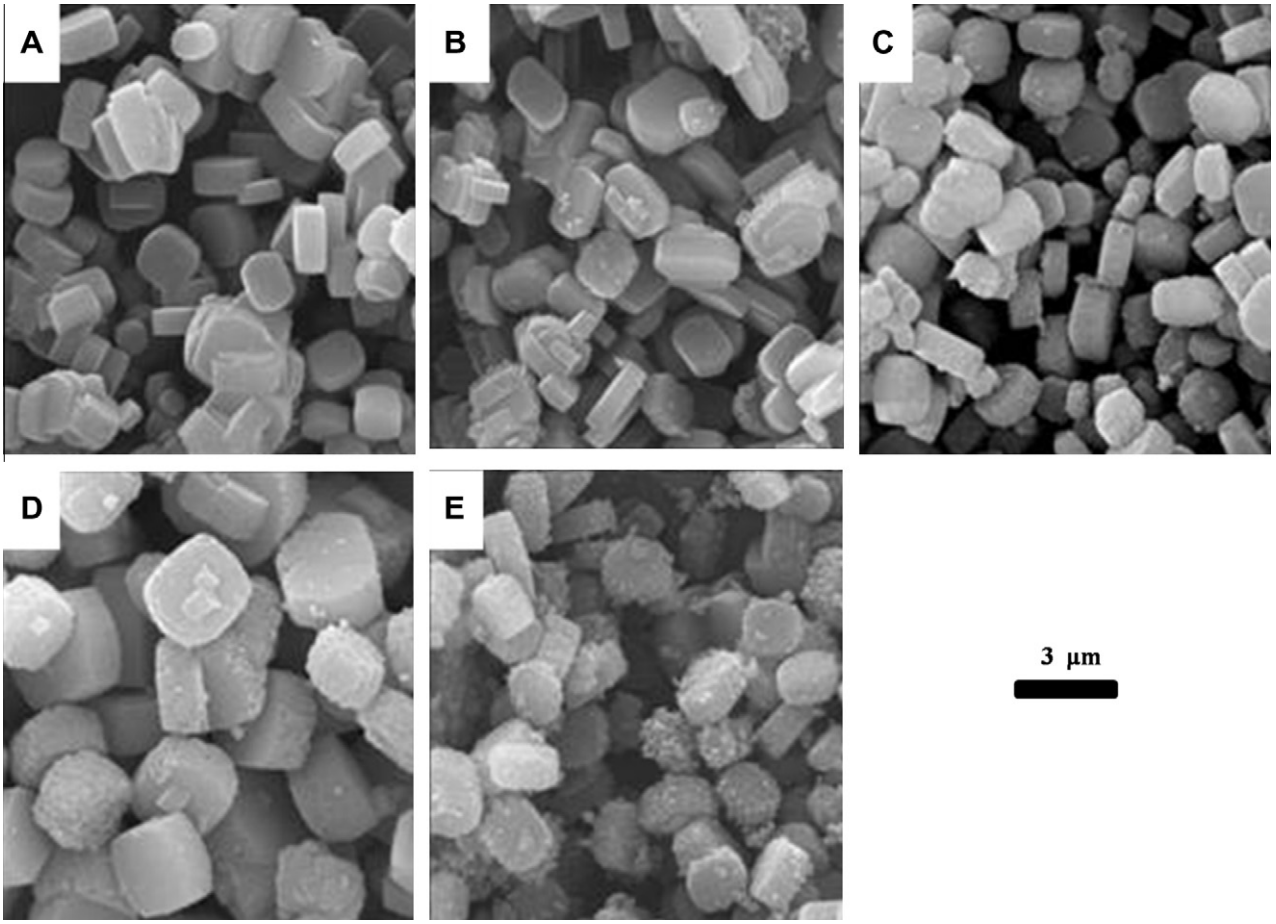

Fig. 4. Scanning electron micrographs of mesoporous ZSM-5 materials synthesized by microwave (A) MW-0, (B) MW-10, (C) MW-20, (D) MW-30, (E) MW-40.

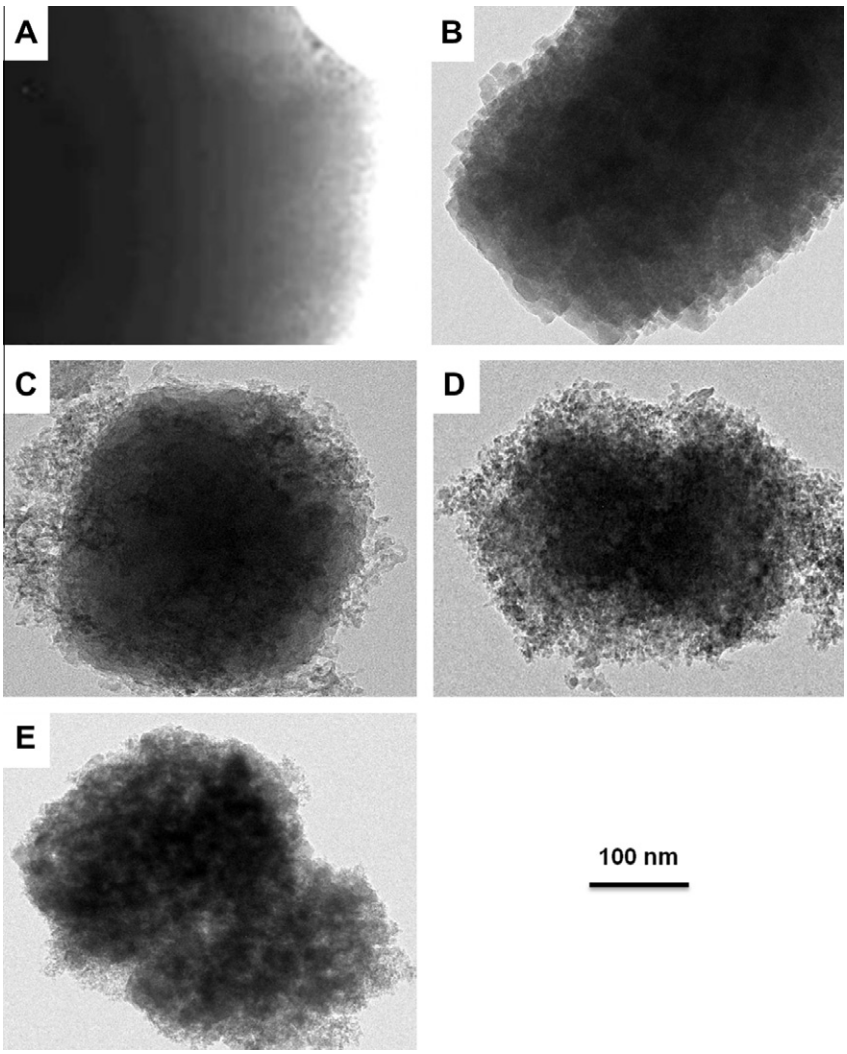

Fig. 5. Transmission electron micrographs of mesoporous ZSM-5 materials synthesized by microwave (A) MW-0, (B) MW-10, (C) MW-20, (D) MW-30, (E) MW-40.

The SEM and TEM images revealed the amount of mesopores from MW-10 to MW-40 increased through the increase of carbon used.

3.4. Incorporation of Al sites

The incorporation of aluminum into mesoporous zeolites synthesized by microwave and hydrothermal methods was confirmed by ^{27}Al MAS NMR as shown in Fig. 6. In ^{27}Al MAS NMR spectra of ZSM-5 samples prepared by microwave (Fig. 6A), a peak centered at 54.4 ppm is clearly seen and can be assigned to tetrahedrally coordinated aluminum in the framework [34]. All spectra clearly indicate the absence of aluminum in octahedral position. ^{27}Al MAS NMR spectra of samples synthesized under hydrothermal conditions (Fig. 6B) showed sharp peak at 54.4 ppm and additional peak at 0 ppm. It means that Al is located in both tetrahedral and octahedral environments in the ZSM-5 zeolite framework. It can be inferred that the microwave played a role to incorporate aluminum into the tetrahedral positions due to a stronger absorption of microwaves by carbon particles. Additionally, from MW-0 to MW-40, the peak at 54.4 ppm was broadened as well as the peak intensity reduced, which was due to the presence of low symmetry aluminum [34,35]. Obviously, more defects will be formed under microwave with increasing amounts of carbon template, and this enhanced the formation of aluminum possessing lower symmetry.

3.5. Acidic properties of mesoporous ZSM-5 catalysts

The acid site distribution on the internal and external surface of the zeolites was investigated using FTIR spectroscopy [35,36]. For that purpose, Py and DTBPy were employed as probe molecules. It is expected that pyridine (kinetic diameter 5.5 Å) can access all acid sites in conventional as well as mesoporous ZSM-5, while DTBPy (kinetic diameter 10.5 Å) is too bulky to penetrate inside the ZSM-5 micropore channel system. DTBPy molecules should only interact with those acid sites located on the external surface of ZSM-5 zeolite crystals or in their pore mouth region [37,38]. As for DTBPy, it is expected that it discriminates the concentrations of Lewis acid sites as tert-butyl groups prevent the interaction with Lewis acid sites. Adsorption of DTBPy leads to the appearance of new absorption band at 1530 cm^{-1}. The band is shifted to lower wavenumbers compared with pyridine, and the absence of the band at 1545 cm^{-1} (pyridine in interaction with Brønsted acid sites) evidences no dealkylation of DTBPy. In this way, only acid sites located at the external surface of medium pore zeolites are evaluated.

In Figs. 7A and 8A, the infrared spectra of all zeolites exhibit two characteristic absorption bands of medium pore zeolites, namely at 3743 cm^{-1} (silanol groups) and 3610 cm^{-1} (bridging Si–OH–Al groups). Despite the different synthesis method used for their preparation, the band widths are rather similar, indicating a

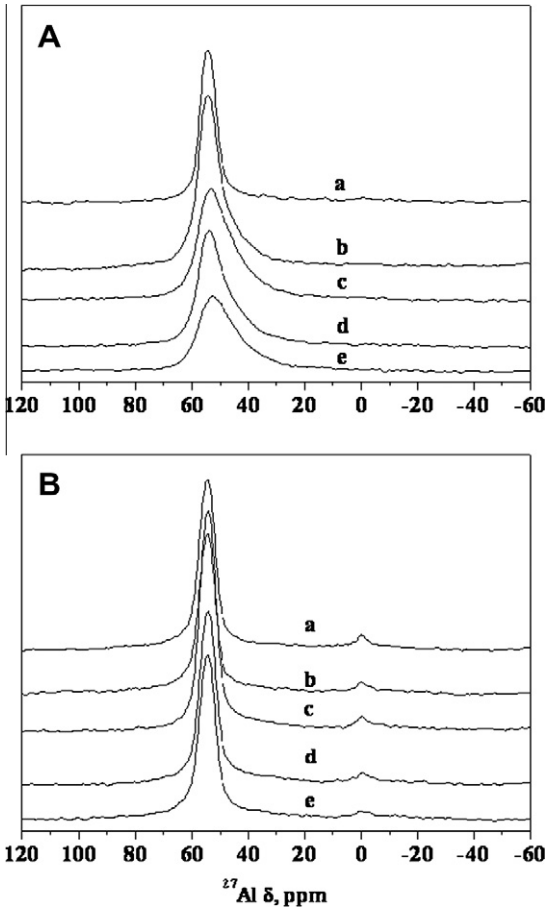

Fig. 6. ^{27}Al-MAS-NMR spectra of mesoporous ZSM-5 synthesized by (A) microwave (a) MW-0, (b) MW-10, (c) MW-20, (d) MW-30, (e) MW-40; (B) hydrothermal (a) HT-0, (b) HT-10, (c) HT-20, (d) HT-30, (e) HT-40.

uniformity of these acidic OH groups [39]. Py adsorption carried out at 150 °C results in the complete disappearance of all acid bridging OH groups (not shown), which evidences that all Si–OH–Al groups are accessible for Py. The interaction of Py with conventional and mesoporous ZSM-5 zeolites leads to the appearance of several new absorption bands at 1545 cm^{-1} and around 1450 cm^{-1} (Figs. 7B and 8B). While the interaction of Py with Brønsted acid sites results in the formation of one new band (1545 cm^{-1}) in all zeolites studied, the interaction of Py with Lewis acid sites leads to the formation of absorption bands at 1445 and 1455 cm^{-1}. The former band is mainly due to Py interacting with silanol groups, and the latter absorption band is typical for pyridine adsorbed on real Lewis acid sites [40].

Based on the intensity of these bands and using molar extinction coefficients [35], the concentrations of Brønsted and Lewis acid sites were determined (see Table 2). These data show some relations among the amount of carbon particles added to the synthesis mixture, way of the preparation of ZSM-5 zeolite and acidic properties. In general, more clear conclusions can be drawn about mesoporous ZSM-5 synthesized under microwave irradiation. First, Si/Al in the zeolite increases with increasing amount of carbon particles in the synthesis mixture. This could indicate that incorporation of aluminum is slowed down under the presence of carbon particles. Concentration of Brønsted acid sites decreases with increasing amount of carbon particles in the synthesis mixture (Table 2). It can be inferred that more defects are formed for higher loading of carbon particles in the synthesis. Decrease in the concentration of Brønsted sites is responsible for the lowering of overall concentration of aluminum in mesoporous ZSM-5 as the amount of Lewis acid sites is more or less independent on the carbon particles in the synthesis mixture. These relationships are less pronounced for mesoporous ZSM-5 prepared under hydrothermal conditions.

Adsorption of DTBPy on zeolites studied does not practically change the shape and the intensity of absorption bands of bridging OH groups. The reason is that the concentration of these groups on the external surface (accessible for DTBPy) is rather low (cf. Table 2). Figs. 7C and 8C show the region of absorption bands of DTBPy interacting with Brønsted acid sites for all conventional and mesoporous ZSM-5 zeolites. This interaction is characterized by an absorption band at 1530 cm^{-1}, while no band around 1450 cm^{-1} was found. It confirms that DTBPy does not adsorb on Lewis acid sites. In this case, the concentrations of Brønsted sites on the external surface increase with the amount of carbon particles in the synthesis gel for both microwave and hydrothermal conditions. Slightly higher amount of "external" acid sites was determined on mesoporous ZSM-5 zeolites prepared under microwave conditions; however, the sample containing 40% of carbon particles synthesized hydrothermally possess the highest amount of Brønsted sites on the external surface.

3.6. Catalytic activity

The textural properties and external acid sites of mesoporous ZSM-5 materials have been correlated with conversion of bimolecular transformation of 2′,4′-dimethoxyacetophenone with

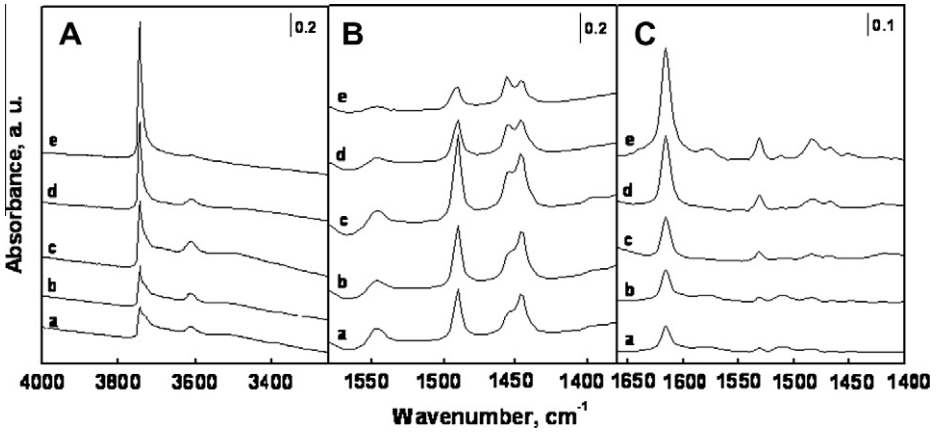

Fig. 7. FTIR spectra of (A) hydroxyl vibration region; (B) spectra of pyridine region; (C) substracted spectra of 2,6-di-tert-butylpyridine region; and in each region (a) MW-0, (b) MW-10, (c) MW-20, (d) MW-30, (e) MW-40.

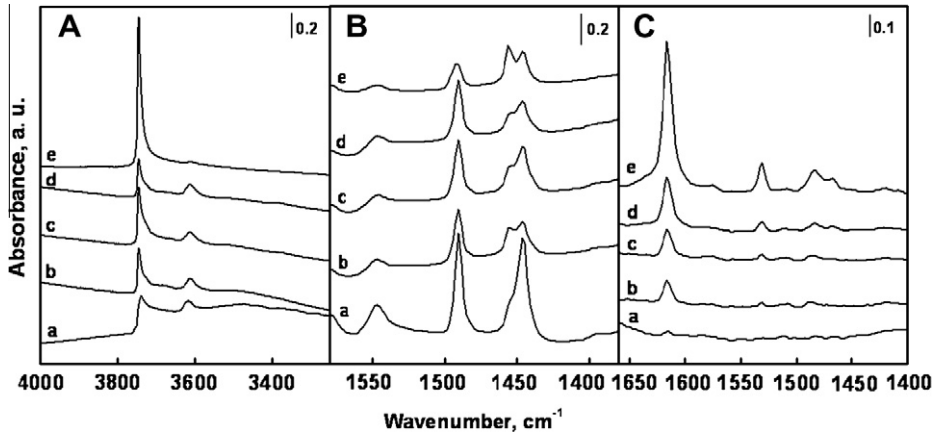

Fig. 8. FTIR spectra of (A) hydroxyl vibration region; (B) spectra of pyridine region; (C) substracted spectra of 2,6-di-tert-butylpyridine region; and in each region (a) HT-0, (b) HT-10, (c) HT-20, (d) HT-30, (e) HT-40.

Table 2
Acid sites distribution on mesoporous ZSM-5 via FTIR of adsorbed pyridine and 2,6-di-tert-butylpyridine.

Samples	Brønsted acid sites (mmol/g)		Brønsted acid sites (%)	
	Overall[a]	Overall[b]	Internal	External
MW-0	0.15	0.03	76.6	23.4
MW-10	0.11	0.04	66.5	33.5
MW-20	0.10	0.04	55.8	44.2
MW-30	0.08	0.05	30.4	69.6
MW-40	0.07	0.07	0.00	100
HT-0	0.22	0.11	67.0	33.0
HT-10	0.23	0.11	67.3	32.7
HT-20	0.24	0.11	69.2	30.8
HT-30	0.23	0.11	67.5	32.5
HT-40	0.25	0.11	69.7	30.3

[a] Calculated from Py adsorption (Figs. 7B and 8B).
[b] Calculated form DTBPy adsorption (Figs. 7C and 8C).

Table 3
Influence of catalysts on conversion of 2′,4′-dimethoxyacetophenone.

Catalysts	Conversion of 2′,4′-dimethoxyacetophenone (%)
MW-40	23.4
MW-0	3.9
HT-40	2.6
HT-0	<1.0

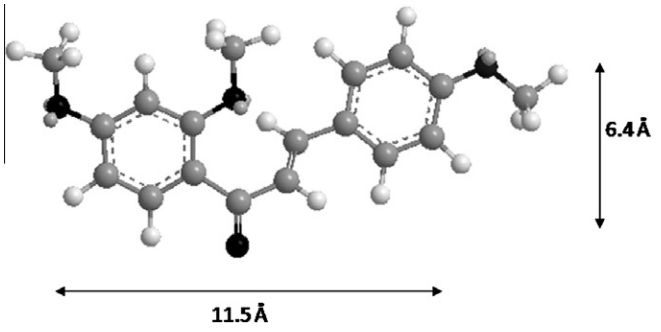

Scheme 2. The energy minimized conformation of vesidryl.

4-methoxybenzaldehyde to vesidryl under solvent-free conditions (Scheme 1). The reaction results are summarized in Table 3. The mesoporous ZSM-5 (MW-40) provided eight times higher conversion than corresponding standard ZSM-5 without mesopores. This is explained by the presence of almost 100% of Brønsted acid sites on the surface of mesopores in the MFI crystals. N_2 sorption studies and FTIR spectra strongly supported the presence of larger amounts of mesopores as well as external Brønsted acid sites, thus resulting in higher conversion of 2′,4′-DMAP over mesoporous ZSM-5 prepared by microwave (MW-40). The typical ZSM-5 synthesized by microwave gave 3.9% conversion of 2′,4′-DMAP, whereas hydrothermal catalysts gave negligible conversion of 2′,4′-dimethoxyacetophenone. The molecular dimension of the product was estimated, and the energy-minimized conformation of product was drawn by using Chem3D Ultra 10.0. The pictorial representation of the energy-minimized conformation of vesidryl is shown in Scheme 2. The size of the product seemed to be larger than pore size of typical ZSM-5. The bulky product could only transport on the mesopore region of the ZSM-5 particles. These observations clearly indicated that the presence of external acid sites in mesopore region was important for the bulky molecular transformation.

Self-condensation of acetophenone has been carried out to identify the role of acidic strength, mesoporosity and mass transfer of substrates. Carbon-templated mesoporous ZSM-5 zeolites synthesized by microwave show much higher conversions of acetophenone in comparison with hydrothermal one as shown in Table 4. There is a gradual increase with increasing carbon content, which is in turn related to the mesoporosity and external acid site. The

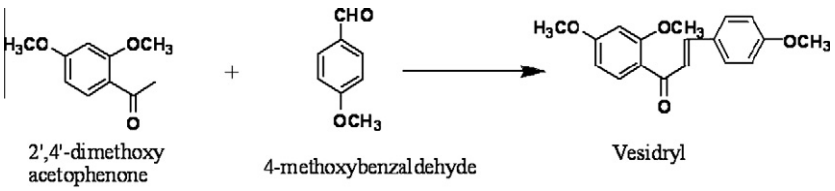

Scheme 1. Synthesis of vesidryl.

Table 4
Self-condensation of acetophenone over mesoporous ZSM-5.

Sample	Conversion (%)	Selectivity (%)	
		trans-Dypnone	Others[a]
C-10% ZSM-5 MW	19.5	83.0	17
C-20% ZSM-5 MW	35.4	84.1	15.9
C-30% ZSM-5 MW	40.6	84.2	15.8
C-40% ZSM-5 MW	42.1	84.4	15.6
C-10% ZSM-5 HT	0.3	98.7	1.3
C-20% ZSM-5 HT	2.3	90.8	9.2
C-30% ZSM-5 HT	2.9	71.1	28.9
C-40% ZSM-5 HT	6.8	77.6	22.4

Reaction condition: 100 mg catalyst was activated @ 100 °C for 2 h, temperature 160 °C, reaction time 5 h, acetophenone 40 mmol.
[a] Others: *cis*-dypnone and ketens.

Table 5
Cracking of 1,3,5-triisopropylbenzene over mesoporous ZSM-5.

	Conv. (%)	Selectivity (%)				
		Benzene	IPB	1,3-DIPB	1,4-DIPB	Others
C-10% ZSM-5 MW	65.8	7.3	5.3	70	8.9	8.5
C-20% ZSM-5 MW	71	2.1	3	80	7.3	7.6
C-30% ZSM-5 MW	78.5	0.77	10.2	82.9	4.4	1.73
C-40% ZSM-5 MW	81.4	0.63	4.5	79.2	4.2	11.47
C-10% ZSM-5 HT	30.3	2.2	0	89.9	0	7.9
C-20% ZSM-5 HT	39.6	5.9	0.53	89	0	4.57
C-30% ZSM-5 HT	63	5.9	1.1	81.7	2.4	8.9
C-40% ZSM-5 HT	73.5	4.4	2.5	78.2	5.28	9.62

Reaction condition: 200 mg catalyst was activated @ 450 °C for 3 h, temperature 400 °C, 1,3,5-triisopropylbenzene 0.2 ml/h, WHSV = 1 h^{-1}.

Al sites were more dispersed in the mesopore wall of ZSM-5 synthesized by microwave method than those hydrothermal method.

The cracking studies of TIPB (1,3,5-triisopropylbenzene) over mesoporous ZSM-5 synthesized by microwave and hydrothermal method show tendency with the amount of carbon content. This reaction strongly depends on the acid site and the amount of mesoporosity. Carbon-templated mesoporous ZSM-5 synthesized by microwave showed higher conversions of TIPB in comparison with hydrothermal one as shown in Table 5, tandem increase is observed with increase in carbon content. The major products in cracking of TIPB were benzene, isopropylbenzene 1,3-diisopropylbenzene and 1,4-diisopropylbenzene, whereas isomerization product 1,4-diisopropylbenzene is mainly observed in microwave-synthesized mesoporous ZSM-5 by isomerization of 1,3-diisopropylbenzene in mesopore. Formation of propylene was not detected due to the off-line analysis.

4. Conclusions

The carbon-templated mesoporous ZSM-5 zeolites have been successfully synthesized under microwave irradiation without drying process. Carbon particles play bifunctional roles as hard template for mesopores and as microwave absorber for Brønsted acid site distribution and zeolite crystallization. By tuning the amount of carbon used, the mesoporosity and acid site distribution could be controlled directly during the preparation. From the quantitative FTIR analysis of pyridine and DTBPy adsorption, it was observed that external acid sites could be varied by amount of carbon template used in the microwave-irradiated synthesis. The MW-40 having 100% Brønsted acid–covered mesopores could catalyze the condensation reaction of 2′,4′-dimethoxyacetophenone with 4-methoxybenzaldehyde effectively.

Acknowledgments

Authors thank financial support of Nano Center for Fine Chemical Fusion Technology from Industry and Energy ministry of Commerce of Korea. M.B. and J.Č. thank the Academy of Sciences of the Czech Republic for the financial support (M200400901).

References

[1] J. Čejka, H. van Bekkum, A. Corma, F. Schűth (Eds.), Introduction to Zeolite Science and Practice, Stud. Surf. Sci. Catal., vol. 168, third ed., Elsevier, Amsterdam, 2007.
[2] A. Corma, Chem. Rev. 95 (1995) 559.
[3] J. Čejka, B. Wichterlová, Catal. Rev. 44 (2002) 375.
[4] W. Vermeiren, J.P. Gilson, Top. Catal. 52 (2009) 1131.
[5] J. Čejka, A. Krejčí, N. Žilková, J. Dědeček, J. Hanika, Micropor. Mesopor. Mater. 44–45 (2001) 499.
[6] P. Prokešová, N. Žilková, S. Mintova, T. Bein, J. Čejka, Appl. Catal. A 281 (2005) 85.
[7] Y. Liu, W. Zhang, T.J. Pinnavaia, Angew. Chem. Int. Ed. 40 (2001) 1255.
[8] D.P. Serrano, J. Aguado, G. Morales, J.M. Rodriguez, A. Peral, M. Thommes, J.D. Epping, B.F. Chmelka, Chem. Mater. 21 (2009) 641.
[9] P. Prokešová, S. Mintova, J. Čejka, T. Bein, Mater. Sci. Eng. C 23 (2003) 1001.
[10] J. Čejka, S. Mintova, Catal. Rev. Sci. Eng. 49 (2007) 457.
[11] J.C. Groen, J.C. Jansen, J.A. Moulijn, J. Pérez-Ramírez, J. Phys. Chem. B 108 (2004) 13062.
[12] J. Pérez-Ramírez, C.H. Christensen, K. Egeblad, C.H. Christensen, J.C. Groen, Chem. Soc. Rev. 37 (2008) 2530.
[13] C. Zhang, Q. Liu, Z. Xu, K. Wan, Micropor. Mesopor. Mater. 62 (2003) 157.
[14] S.-S. Kim, J. Shah, T.J. Pinnavaia, Chem. Mater. 15 (2003) 1664.
[15] N. Viswanadham, M. Kumar, Micropor. Mesopor. Mater. 92 (2006) 31.
[16] C.J.H. Jacobsen, C. Madsen, J. Houzvicka, I. Schmidt, A. Carlsson, J. Am. Chem. Soc. 122 (2000) 7116.
[17] A. Sakthivel, S.J. Huang, W.-H. Chen, Z.-H. Lan, K.-H. Chen, T.-W. Kim, R. Ryoo, A.S.T. Chiang, S.-B. Liu, Chem. Mater. 16 (2004) 3168.
[18] Y. Tao, H. Kanoh, K. Kaneko, J. Am. Chem. Soc. 125 (2003) 6044.
[19] Y. Tao, Y. Hattori, A. Matumoto, H. Kanoh, K. Kaneko, J. Phys. Chem. B 109 (2005) 194.
[20] S.-E. Park, J.-S. Chang, Y.-K. Hwang, D.-S. Kim, S.-H. Jhung, J.-S. Hwang, Catal. Surv. Asia 8 (2004) 91.
[21] G.A. Tompsett, W.C. Conner, K.S. Yngvesson, Chem. Phys. Chem. 7 (2006) 296.
[22] C.S. Cundy, Collect. Czech. Chem. Commun. 63 (1998) 1699.
[23] B.L. Newalkar, H. Katsuki, S. Komarneni, Micropor. Mesopor. Mater. 73 (2004) 161.
[24] S. Abelló, J. Pérez-Ramírez, Phys. Chem. Chem. Phys. 11 (2009) 2959.
[25] Y.K. Hwang, J.-S. Chang, S.-E. Park, D.S. Kim, Y.-U. Kwon, S.H. Jhung, J.-S. Hwang, M.S. Park, Angew. Chem. Int. Ed. 44 (2005) 556.
[26] N. Jiang, D.-S. Han, S.-E. Park, Catal. Today 141 (2009) 344.
[27] D.A. Makeiff, T. Huber, Synth. Metal 156 (2006) 497.
[28] J.P. Calame, W.G. Lawson, IEEE Trans. Elect. Dev. 38 (1991) 1538.
[29] K. Egeblad, M. Kustova, S.K. Klitgaard, K. Zhu, C.H. Christensen, Micropor. Mesopor. Mater. 101 (2007) 214.
[30] M. Kustova, K. Egeblad, C.H. Christensen, A.L. Kustov, C.H. Christensen, Stud. Surf. Sci. Catal. 170 (2007) 267.
[31] K.M. Jinka, S.-C. Lee, S.-E. Park, R.V. Jasra, Stud. Surf. Sci. Catal. 174 (2008) 1187.
[32] K. Egeblad, C.H. Christensen, M. Kustova, C.H. Christensen, Chem. Mater. 20 (2008) 946.
[33] A. Zukal, H. Šiklová, J. Čejka, Langmuir 24 (2008) 9837.
[34] D. Trong-On, A. Nossov, S.-H. Marie-Anne, C. Schneider, J.L. Bretherton, C.A. Fyfe, S. Kaliaguine, J. Am. Chem. Soc. 126 (2004) 14324.
[35] B. Gil, S.I. Zones, S.J. Hwang, M. Bejblová, J. Čejka, J. Phys. Chem. C 112 (2008) 1997.
[36] P. Nachtigall, O. Bludský, L. Grajciar, D. Nachtigallová, M.R. Delgado, C.O. Areán, Phys. Chem. Chem. Phys. 11 (2009) 791.
[37] A. Corma, V. Fornes, L. Forni, F. Márquez, J. Martínez-Triguero, D. Moscotti, J. Catal. 179 (1998) 451.
[38] S. Zheng, H.R. Heydenrych, A. Jentys, J.A. Lercher, J. Phys. Chem. B 106 (2002) 9552.
[39] J. Datka, B. Gil, J. Mol. Struct. 596 (2001) 41.
[40] J. Datka, B. Gil, J. Złamaniec, P. Batamack, J. Fraissard, P. Massiani, Polish J. Chem. 73 (1999) 535.